Inherent Photodegradability of Polymethacrylate Hydrogels: Straightforward Access to Biocompatible Soft Microstructures

Lei Li, [a] *Johannes M. Scheiger,* [a] *Tina Tronser,* [a] *Connor Long,* [b] *Konstantin Demir,* [a] *Christina L. Wilson,* [b] *Mariia A. Kuzina,* [c] *and Pavel A. Levkin** [a, d]

J. M. Scheiger, Dr. T. Tronser, K. Demir, Dr. P. A. Levkin
Institute of Toxicology and Genetics (ITG), Karlsruhe Institute of Technology (KIT), 76021 Karlsruhe, Germany

C. Long, Dr. C. Wilson
Department of Chemistry, Doane University, 1014 Boswell Ave, Crete, NE 68333, United States

M. Kuzina
Department of Materials Science, L. Moscow State University
Leninskie Gory, Moscow, 119991, Russian Federation

Dr. P. A. Levkin
Institute of Organic Chemistry, KIT, 76131 Karlsruhe

Dr. L. Li
Key Laboratory of Special Functional Aggregated Materials
Ministry of Education, School of Chemistry and Chemical Engineering, Shandong University, Jinan 250100, P. R. China

E-mail: levkin@kit.edu

Keywords: ((photodegradable hydrogels, hydrogel patterns, cell aggregates, photochemistry))

Hydrogels are important functional materials useful for three-dimensional (3D) cell culture, tissue engineering, 3D printing, drug-delivery, sensors or soft-robotics. The ability to shape hydrogels into defined three-dimensional structures, patterns or particles is crucial for biomedical applications. Here, the rapid photodegradability of commonly used polymethacrylate hydrogels is demonstrated without the need to incorporate additional photolabile functionalities. Hydrogel degradation depths were quantified in respect of the irradiation time, light intensity, and chemical composition. It could be shown that these parameters can be utilized to control the photodegradation behavior of polymethacrylate hydrogels. The photodegradation kinetics, the change of mechanical properties of polymethacrylate hydrogels upon UV irradiation as well as the photodegradation products have

been investigated. This approach was then exploited for microstructuring and patterning of hydrogels including hydrogel gradients as well as for the formation of hydrogel particles and hydrogel arrays of well-defined shapes. Cell repellent but biocompatible hydrogel microwells were fabricated using this method and used to form arrays of cell spheroids. As this method is based on readily available and commonly used methacrylates and can be conducted using cheap UV light sources, it has vast potential to be applied by labs with various backgrounds and for diverse applications.

1. Introduction

Hydrogels are water-swollen three-dimensional (3D) networks of either physically or chemically crosslinked hydrophilic polymers.[1] Their unique tuneable physical properties, structure and biocompatibility, mimicking those of tissues and cellular microenvironment, made them an important, versatile soft material useful for various applications in biotechnological and biomedical fields, including actuators,[2] sensors,[3] artificial muscles,[4] drug delivery,[1a] and tissue engineering.[5] These and many other applications require hydrogels with well-defined chemical and physical properties, shape, topography, mechanical properties, porosity and biocompatibility.[6]

Several types of photodegradable hydrogels have been introduced in literature to prepare microstructured soft materials or to define chemical and physical properties with spatiotemporal control.[7] However, to achieve hydrogel photodegradability, artificial photoresponsive units or crosslinkers had to be synthesized and incorporated into the hydrogel network, which would then serve as breaking points under UV light. Such photodegradable moieties include *o*-nitrobenzyl ester,[8] coumarins,[9] disulfides,[10] Ru^{II} polypyridyl complexes,[11] etc. The limited number of available photolabile groups and the need for their synthesis and incorporation into the hydrogel network significantly limit the number and scope of possible applications of photodegradable hydrogels for a broader audience. Here we demonstrate, for the first time, that

one of the most commonly used types of hydrogels, i.e. hydrogels based on hydrophilic polymethacrylates, can be efficiently degraded using UV light without requiring any external photolabile moieties (**Figure 1**A). The different methacrylate-based monomers and crosslinkers used in this study are shown below (Figure 1B). This opens the possibility to use conventional photolithographic methods to structure hydrogels, i.e. create complex hydrogel patterns, hydrogel particles or hydrogel gradients utilizing various types of commercially available hydrophilic methacrylate monomers and crosslinkers (Figure 1C). Interestingly, produced hydrogel particles still exhibit photodegradability and could be completely degraded by further UV irradiation (Figure S3).

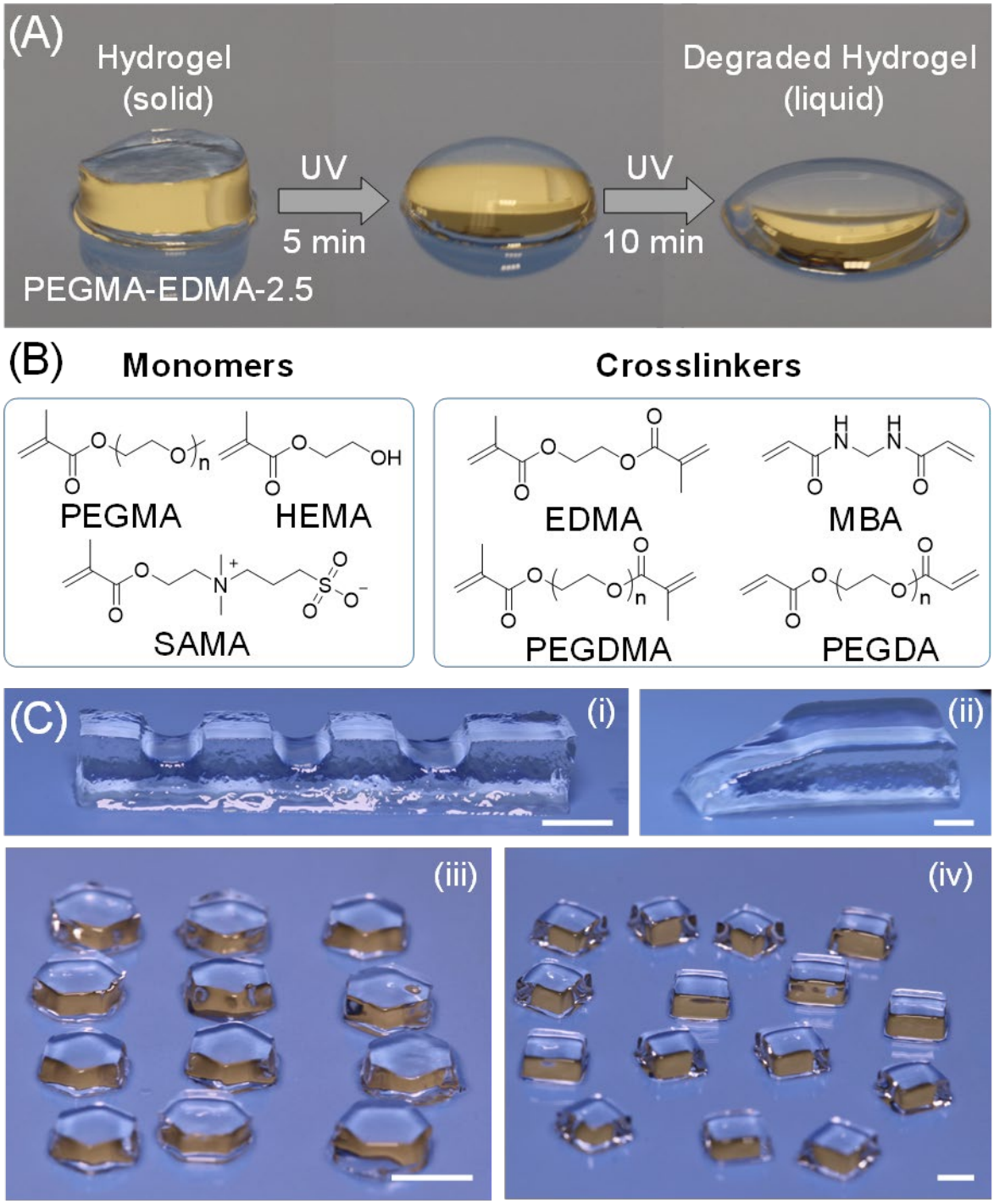

Figure 1. (A) Time-lapse images of a 3 mm-thick hydrogel block ($PEG_{500}MA$-EDMA-2.5) exposed to UV irradiation (2 mW/cm^2). (B) Molecular structures of monomers and crosslinkers used for the formation of inherently photodegradable hydrogels (C) Digital images of hydrogel channels (I), hydrogels with thickness gradient (by moving the photomask during UV irradiation) (II) and free-standing hydrogel particles (III, IV). Scale bars are 5 mm.

UV irradiation of polymethacrylates that do not contain any photoresponsive groups can cause homolysis of main chain carbon-carbon bonds leading to photodegradation.[12] There are three known routes for the photolysis process: direct main-chain scission, main-chain scission following side-chain scission, and photo-oxidative main chain scission.[13] The inherent UV vulnerability of polymethacrylates such as PMMA has been known for several decades. Surprisingly, to the best of our knowledge, the inherent photodegradability of polymethacrylates has rarely been exploited as an advantage before and there are no reports about the inherent photodegradability of polymethacrylate hydrogels, despite their wide use in industry and research as well as the importance of hydrogel microengineering.

2. Results and Discussion

2.1 Polymethacrylate Hydrogel Synthesis and UV Structuring

We synthesized various polymethacrylate hydrogels via radical polymerization of various methacrylates and crosslinkers initiated by ammonium persulfate (9.2 mM) and *N,N,N',N'*-tetramethylethylenediamine (12 mM). The obtained hydrogels are termed 'monomer-crosslinker-X%', where X% equals to $n_{crosslinker}/(n_{crosslinker}+n_{monomer})*100\%$, with the concentration of the monomer and crosslinker fixed at 20 wt%. In this study, we investigated three kinds of monomers, poly(ethylene glycol) methyl ether methacrylate (M_n 500, $PEG_{500}MA$), (hydroxyethyl)-methacrylate (HEMA), [2-(methacryloyloxy)ethyl]dimethyl-(3-sulfopropyl) ammonium hydroxide (SAMA) and four different crosslinkers, ethylene glycol dimethacrylate (EDMA), *N,N'*-methylene bisacrylamide (MBA), poly(ethylene glycol) dimethacrylate, (M_n 4000, $PEG_{4000}DMA$) and poly(ethylene glycol) diacrylate (M_n 700, $PEG_{700}DA$). To test the photodegradability, 3 mm-thick hydrogel samples were exposed to UV light (260 nm, 2 mW/cm^2). As seen in Figure 1A, UV irradiation leads to fast and complete degradation of hydrogels. Minimum exposure times for 3 mm thick hydrogels for complete

liquification ranged from 10 min to 30 min, depending on the chemical composition of hydrogel samples (Figure S4).

The process of formation and degradation was followed up with ^{13}C-NMR and ^{1}H-NMR in a step wise manner by exchanging water in the prepolymerization mixture with D_2O and polymerizing the sample directly in an NMR tube (**Figure 2**A, S14). Characteristic peaks of the starting materials, such as both vinyl proton and carbon peaks, disappeared quantitatively. After UV photodegradation new peaks emerged, which could be assigned to poly(ethylene) glycol formate (PEG formate) moieties. This indicates the occurrence of side chain cleavages, which might contribute to the main-chain degradation mechanism (for full spectra see Figure S14-17). Rheometry data provided quantitative insight into the photodegradation process. PEG_{500}MA-EDMA-10 hydrogel was selected as model sample (Figure S5). The storage modulus (G') of PEG_{500}MA-EDMA-10 hydrogel is frequency independent and more than one order of magnitude greater than its loss modulus (G''), indicating a crosslinked sample.[14] Upon irradiation with UV light (260 nm, 5 mW/cm^2), the G' of the hydrogel gradually decreased from 280 Pa to 84 Pa, resulting in a 57% loss of the original storage modulus (G'_0), after 7 min exposure. Longer irradiation led to the total degradation of the hydrogel.

To investigate the photodegradation speed, we monitored the change of hydrogel thickness along with the UV irradiation time. PEG_{500}MA-EDMA-10 hydrogels were exposed to masked UV light to show the contrast between exposed areas and unexposed areas. After irradiation, hydrogel samples were stained with Rhodamine B to measure the hydrogel thickness with confocal fluorescence microscopy. The hydrogel thickness significantly decreased in the exposed areas, whereas the unexposed regions remained intact (Figure 2B). The progressively recessed features indicate that the photodegradation is a surface erosion process. We assume that the UV light intensity gradually decreases along the light path in the hydrogel due to light absorption which causes the uppermost layers of a hydrogel to erode first under UV irradiation.

To investigate factors influencing the photodegradation speed, flat hydrogels were exposed to flood irradiation for different times and their erosion depths were measured with optical microscopy. It was found that a higher UV intensity led to faster hydrogel erosion (Figure 2C). For a photodegradable hydrogel with a fixed composition, we can therefore define the photodegradation depth by adjusting the UV exposure time and tailor the erosion kinetics by altering the UV intensity.

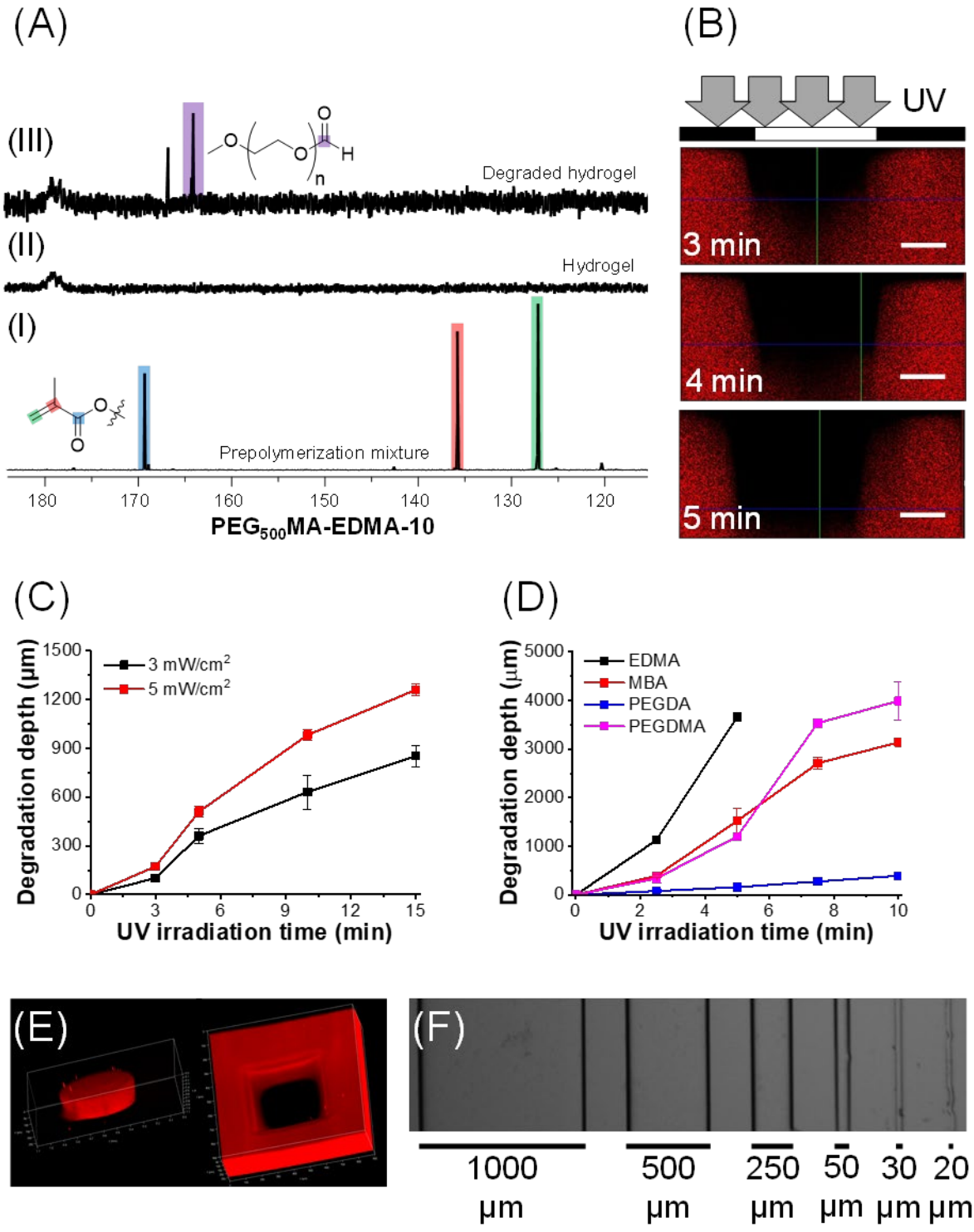

Figure 2. (A) ^{13}C-NMR spectra of $PEG_{500}MA$-EDMA-10 prepolymerization mixture and the respective polymerized hydrogel and photodegraded (260 nm, 4 mW/cm^2) hydrogel solution. The disappearance of vinyl peaks (red and green) from (I) to (II) proved full conversion of monomer and crosslinker. Newly arising peaks in (III) indicate formation of poly(ethylene glycol) formate, a product of UV induced side-chain cleavages.(B) Fluorescence microscopy

images of progressively recessed $PEG_{500}MA$-EDMA-10 hydrogel (red) over 5 minutes of UV irradiation (260 nm, 5 mW/cm^2). Scale bars are 200 μm. (C) Photodegradation kinetics of the $PEG_{500}MA$-EDMA-10 hydrogel exposed to UV light with different intensities. (D) Effect of crosslinkers on the photodegradation kinetics of PEGMA-crosslinker-2.5 hydrogels. Crosslinkers used were ethylene glycol dimethacrylate (EDMA), N,N'-methylene bisacrylamide (MBA), and poly(ethylene glycol) dimethacrylate (M_n 700, $PEG_{700}DA$). The amount of the crosslinker poly(ethylene glycol) dimethacrylate (M_n 4000, $PEG_{4000}DMA$) had to be decreased to 0.17 mol% to achieve the apparent photodegradation kinetics under the same conditions (260 nm, 5 mW/cm^2). (E) 3D hydrogel shapes by confocal microscopy. Scale bars are 500 μm. (F) Brightfield microscope images of 12.5 μm-thin $PEG_{500}MA$-EDMA-10 hydrogel patterns with lines of different widths. The smallest features that could be produced were ~20 μm.

We further investigated the effect of chemical composition of hydrogels on their photodegradation behavior. Faster degradation was achieved by reducing the amount of EDMA from 10 mol% to 2.5 mol%. We attribute the increased speed of degradation for X = 2.5 mol% to the decreased amount of crosslinking. To test the effects of crosslinker chemistry on the photodegradation kinetics, hydrogels were prepared by copolymerization of $PEG_{500}MA$ with different crosslinkers (Figure 2D): MBA, $PEG_{700}DA$, $PEG_{4000}DMA$. Holding constant the gelation/irradiation conditions and the ratio of crosslinker to monomer, the $PEG_{500}MA$-$PEG_{700}DA$-2.5 hydrogel showed the slowest degradation with an erosion depth of 150 μm after 5 min, while $PEG_{500}MA$-MBA-2.5 hydrogel and $PEG_{500}MA$-EDMA-2.5 hydrogel demonstrated 1500 μm and 3650 μm of degradation, respectively. Different crosslinkers resulted in different cross-linking degrees in hydrogels which required more UV energy to de-crosslink the network. This hypothesis was supported by the fact that $PEG_{500}MA$-$PEG_{4000}DMA$-2.5 did not show apparent degradation even after 10 min, while fast

photodegradation was observed when the ratio of $PEG_{4000}DMA$ was decreased from 2.5 mol% to 0.17 mol%. To demonstrate the proposed general applicability of this method amongst methacrylate monomers, hydrogels based on (2-hydroxyethyl)methacrylate (HEMA) and [2-(methacryloyloxy)ethyl]dimethyl-(3-sulfopropyl)ammonium (SAMA) were fabricated. In detail, ($HEMA_{80m\%}$-$PEG_{500}MA_{20m\%}$)-EDMA-0.85 and SAMA-EDMA-2.5 hydrogels were studied. Since polyHEMA has limited solubility in water, 20 mol% of $PEG_{500}MA$ had to be copolymerized with HEMA to avoid phase separation. Both hydrogels showed photodegradability (Figure S5-S9) in a controllable way. Therefore, it seems likely that this method can be extended to other methacrylates. A key advantage of a surface erosion process is the ability to form precise 3D microstructures, such as microwells or microchannels within hydrogels without sacrificing the integrity of the hydrogel in bulk. The controllable kinetics (via light intensity, choice of crosslinker and monomer, relative amount of crosslinker) and spatial control of the photodegradation process thus made it possible to fabricate hydrogel micropatterns, structured hydrogel surfaces or hydrogel microparticles with defined shapes and sizes. To demonstrate this, we subjected $PEG_{500}MA$-EDMA-10 hydrogel thin films to UV light through different photomasks and visualized the result with confocal microscopy (Figure 2E). Well-defined arrays or meshes of hydrogel structures with different geometries could be obtained as well (Figure S10). To investigate the resolution limit of this fabrication technique, we patterned a 12.5 μm-thin $PEG_{500}MA$-EDMA-10 hydrogel layer with different feature sizes. Hydrogel microstructures with dimensions down to 20 μm could be fabricated (Figure 2F).

2.2 Polymethacrylate Hydrogel UV Photodegradation

To investigate the UV photodegradation microscopically, we chose $PEG_{500}MA$-EDMA-10 as a model system. The vulnerability of poly(meth)acrylate homopolymers towards UV light in previous studies was examined in bulk (films) or in solution and investigated in dependence of wavelength[15] and monomers.[16] Most studies were conducted to gain insight about the lifetime

of homopolymer´s upon exposure to sunlight or their usefulness as photoresist.[17] Two major processes caused by UV irradiation were identified: Photoinduced degradation and -crosslinking, with the amount crosslinking being quantified simply by determining the mass of the insoluble fraction forming from a former soluble homopolymer.[18] It was found that polyacrylates tend to crosslink more than the respective polymethacrylates and that longer aliphatic ester side chains resulted in more photocrosslinking. This finding was related to the lower glass transition temperatures (T_g) of polymethacrylates with longer ester side chains, resulting in a higher mobility of macroradicals formed via UV.[19] Thus, we hypothesize that due to the use of hydrophilic polymethacrylates in a swelled hydrogel state, the photodegradation is a lot more efficient than in bulk due to suppression of the competing crosslinking reaction, arising from the spatial separation of polymer chains and the restricted mobility of macroradicals. This hypothesis was supported by the observation that dried out PEG_{500}MA-EDMA-10 hydrogels did not show degradation under UV light. A similar effect was described by Grassie for the photodegradation of poly(methyl methacrylate)-*co*-(methyl acrylate) in solution.[20] Indeed, we report degradation times on the minute scale, whereas the degradation experiments performed on bulk materials were conducted in the range of hours to hundreds of hours before even surface degradation effects became apparent. Another reason for the fast degradation of polymethacrylate hydrogels could be the diffusion of soluble network fragments from the surface into the bulk hydrogel, enabling a more efficient ablation. UV photodegradation in previous studies resulted in slight changes in the respective UV-Vis and FTIR spectra or a decrease in the molecular weight. It was found that photodegradation does not occur above UV wavelengths of ca. 310-320 nm.[21] This behavior is confirmed for the model hydrogel PEG_{500}MA-EDMA-10 with degradation experiments using a <320 nm filter (Figure S11). DLS and SEC measurements confirm the presence of soluble polymer chains after irradiation of PEG_{500}MA-EDMA-10 hydrogels (Figure S12) with UV light. Both

techniques show decreasing values for molecules size and weight with increasing irradiation time (**Table 1**).

Table 1. DLS and SEC data for $PEG_{500}MA$-EDMA-10 hydrogels irradiated for different times.

Irradiation time [min]	Size average [nm]	M_n [kDa]	M_w [kDa]
15 min	110.2 ± 2	n/a	n/a
30 min	39.4 ± 0.8	n/a	n/a
45 min	27.9 ± 0.5	20.4	49.9
60 min	20.7 ± 0.2	14.8	42.1
75 min	n/a	13.6	30.4
90 min	n/a	11.0	28.1
120 min	n/a	7.2	13.0

High molecular weight polymer chains disappeared faster and the molecular weight distribution (MWD) narrowed upon irradiation, hinting towards a random chain scission mechanism. A similar narrowing of the MWD upon UV irradiation of PMMA was reported by Caykara et al.[22] In the ^{13}C-NMR (Figure 2A and Figure S16-19) of degraded $PEG_{500}MA$-EDMA-10 hydrogels we observed the appearance of peaks that could be attributed to PEG formate, PEG peroxides and PEG hydroperoxides. Therefore, we assumed that UV induced side chain scissions take place, which contribute to the main-chain degradation mechanism. The degradation derived soluble $PEG_{500}MA$ polymer showed typical LCST behavior (Figure S13). Our observed cloud point at around 80 °C is in the range of values reported for homopolymers of $PEG_{475}MA$.[23] Further support for our claim of a hydrogel network degrading into non-crosslinked soluble polymer chains is provided by SEM (Figure S18). Via masked irradiation, a pristine and a photodegraded $PEG_{500}MA$-EDMA-10 hydrogel could be compared in a single SEM image. While the pristine $PEG_{500}MA$-EDMA-10 network had a porous microstructure, the degraded part had a smooth surface topology, as expected for linear polymer chains.

2.3 UV Microstructured Polymethacrylate Hydrogel as Bioscaffolds

The most relevant hydrogel applications are biorelated. Precisely shaped hydrogel particles are used for applications in biomaterials,[24] biosensing,[25] drug delivery,[26] and photonic materials.[27] Simple and broadly applicable structuring tools are thus highly desired.[28]

Our method demonstrated to be feasible for 3D cell culture, for which we could rapidly fabricate hydrogel scaffolds. In recent years, 3D cell culture has revolutionized our understanding of cellular behavior and involved areas of cell biology, drug screening, tissue engineering.[29] Compared with the traditional two-dimensional (2D) models, 3D models can better mimic both chemical and physical cues of native cellular microenvironment and allow for the cell-cell and cell-ECM signaling, important for cell growth, proliferation, differentiation, and other cellular functions.[30] The photodegradable hydrogels reported here provide a very convenient access to hydrogel surfaces with arrays of biocompatible but cell repellent cavities with defined shape and depth that can be used for the formation of arrays of three-dimensional cellular clusters, spheroids or embryoid bodies. The use of PEG-based hydrogels ensured resistance to cell adhesion, which is crucial for the growth of 3D cell clusters.[31] We evaluated this system for the formation of 3D multicellular aggregates using mouse embryonic stem cells (mESCs) and human cervical tumor cells (HeLa).[32]

Cylindrical microwells were fabricated by photopatterning 125 µm-thick $PEG_{500}MA$-$PEG_{700}DA$-2.5 hydrogel (Figure 3A). Confocal microscopy images demonstrated the 3D structure of the hydrogel microwells with depth of 60 µm and diameter of 100 µm (Figure 3C). After the microwell array was sterilized in ethanol and equilibrated with PBS, Hela cells were seeded onto the hydrogel surface at a density of $1*10^5$ cells/mL and allowed them to settle into the microwells for 5 minutes before the arrays were gently washed to remove the excess of cells located outside of the microwells. Brightfield images show cells trapped within each circular microwell. During the 7-day incubation, the increasing of cell density indicates cell proliferation, demonstrating the cytocompatibility of this hydrogel (Figure 3B). From day 3

onward, Hela cells began to aggregate in each microwell. After 7 days, Hela cells grew to fill the full volume of microwells and formed uniform cell aggregates. Both the periphery and the bottom surface of the microwells are cell-repellent due to the PEG hydrogel, which promotes cell-cell contacts and thus multi-cellular aggregate formation. Very high cell viabilities (after 7 days incubation) were assessed by staining dead cells with propidium iodide (PI) and nuclei with Hoechst (Figure 3D). Confocal fluorescence images confirmed the compact 3D structure of cell aggregates (Figures 3E, 3F), with diameter of 100 µm and height of 50 µm scaled with the microwell dimensions. Using this scaffold, cell aggregates of other geometries are easily accessible by culturing cells in microwells with corresponding patterns. Thus, cubic Hela cell aggregates could be formed in square hydrogel cavities with 200 µm side and 60 µm heights (Figures 3G, 3H and S20).

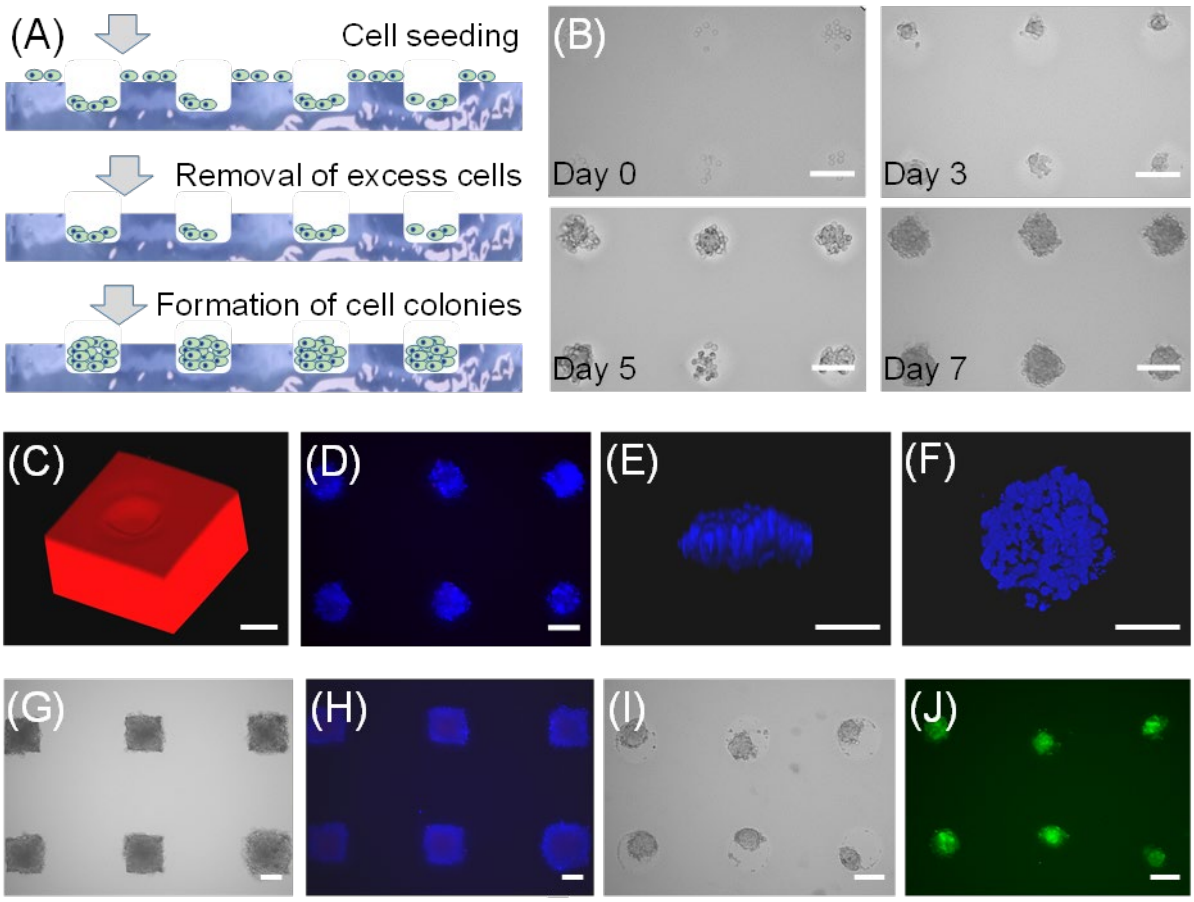

Figure 3. (A) Schematic formation of arrays of cavities in a $PEG_{500}MA$-$PEG_{700}DA$-2.5 hydrogel layer for 3D cell culture. (B) Brightfield microscopy images of human cervical tumor

cells (Hela) cultured in the hydrogel microwells for 7 days to form dense 3D cell aggregates. (C) Confocal microscopy image of a microwell. (D) Overlay fluorescence images of both Hoechst (blue) - and propidium iodide (PI, red) stained cell aggregates after 7 day incubation within the microwells. (E) Side view and (F) superior view of the formed cell aggregate. (G) Brightfield image shows the cube Hela cell aggregates after 10-day incubation and high cell viability is supported by the overlay (H) fluorescence images of both Hoechst- and PI- stained cell aggregates. (I) Mouse embryonic stem cells (mESCs) aggregates in circular hydrogel microwell arrays. Brightfield image shows mESCs formed dense aggregates and the (J) fluorescence image of GFP indicates the maintenance of stemness of mESCs up to two days. Scale bars: 100 μm for B, C, D, G, H, I and J; 50 μm for E and F.

To demonstrate the broad applicability of this strategy, we further used this scaffold to fabricate stem cell aggregates. A transgenic mouse embryonic stem cell line with green fluorescent protein (GFP) stably fused to Oct4 (mESC Oct4-eGFP) was used in this study. This cell line permits the rapid characterization of stemness by examining the fluorescence related with expression levels of the Oct4-eGFP reporter gene.[33] mESCs were seeded into the circular microwell array and incubated for 6 days. During this period, mESCs proliferated and formed dense aggregates, showing the same shape as that of the microwell array (Figures 3I, 3J and S20A). High cell viability was also achieved (Figure S21B). The solution resulting from photodegradation of the model hydrogel PEG_{500}MA-EDMA-10 could be shown to be harmless to cells in most concentrations (Figure S19). Interestingly, we found the GFP fluorescence increased in the first two days (Figures 3I and 3J) and gradually decreased after the third day (Figure S21A), indicating that the hydrogel microwell array promotes the maintenance of stemness of mESCs up to two days, while longer incubation will lead to the differentiation of mESCs. However, further experiments are required to illustrate the mechanism of this

phenomenon. These size-controlled cell aggregates could be useful for in vitro high throughput studies of tumor development and stem cell behaviors as well as in drug screening studies.

To summarize, hydrogels are extremely important biomimetic materials useful in biomedicine, biotechnology, tissue engineering, drug delivery and many other research fields. Here, we demonstrated that commonly used methacrylate hydrogels can be efficiently and rapidly degraded by UV irradiation. This opens uniquely simple possibilities for creating structured hydrogel films, hydrogel micropatterns or hydrogel particles based on frequently used tunable and biocompatible polymethacrylates. We showed the suitability of our method for bioapplications by creating an array of cell repellent but biocompatible microwells in a hydrogel layer to form arrays of three-dimensional cellular aggregates. It could be demonstrated that such photodegradability is inherent to various types of methacrylate hydrogels based on different hydrophilic methacrylates monomers and crosslinkers in innumerable compositions. The degradation processes were quantified macroscopically and investigated microscopically. A simple and versatile method for patterning and structuring of hydrogels was introduced, which provides easy access to diversely structured hydrogels opening vast opportunities for research and novel applications of this ubiquitous class of materials.

Supporting Information is available from the Wiley Online Library or from the author.

Acknowledgements
L. L. and J.S. contributed equally to this work. The authors acknowledge the help of Lukas Arens from the group of Manfred Wilhelm (KIT) with the rheological measurements. The research was supported by the ERC Starting Grant (337077-DropCellArray), Helmholtz Association's Initiative and Networking Fund (HGF-ERC–0016), National Science Foundation (Grant No. 1459838) and National Institute for General Medical Science (NIGMS, 5P20GM103427).

Received: ((will be filled in by the editorial staff))
Revised: ((will be filled in by the editorial staff))
Published online: ((will be filled in by the editorial staff))

References

[1] a) A. S. Hoffman, *Adv. Drug Del. Rev.* **2012**, *64*, 18; b) A. S. Hoffman, *Adv. Drug Del. Rev.* **2002**, *54*, 3; c) J. A. Burdick, W. L. Murphy, *Nat. comm.* **2012**, *3*, 1269.

[2] J. Kim, J. A. Hanna, M. Byun, C. D. Santangelo, R. C. Hayward, *Science* **2012**, *335*, 1201.

[3] Y. J. Heo, H. Shibata, T. Okitsu, T. Kawanishi, S. Takeuchi, *Proc. Natl. Acad. Sci. U.S.A.* **2011**, *108*, 13399.

[4] C. Larson, B. Peele, S. Li, S. Robinson, M. Totaro, L. Beccai, B. Mazzolai, R. Shepherd, *Science* **2016**, *351*, 1071.

[5] M. P. Lutolf, J. A. Hubbell, *Nat. biotech.* **2005**, *23*, 47.

[6] Y. S. Zhang, A. Khademhosseini, *Science* **2017**, *356*.

[7] a) A. M. Rosales, S. L. Vega, F. W. DelRio, J. A. Burdick, K. S. Anseth, *Angew. Chem. Int. Ed.* **2017**, *56*, 12132; b) E. R. Ruskowitz, C. A. DeForest, *Nat. Rev. Mater.* **2018**, *3*, 17087; c) C. Siltanen, D.-S. Shin, J. Sutcliffe, A. Revzin, *Angew. Chem. Int. Ed.* **2013**, *52*, 9224; d) F. Yanagawa, S. Sugiura, T. Takagi, K. Sumaru, G. Camci-Unal, A. Patel, A. Khademhosseini, T. Kanamori, *Adv. Healthc. Mater.* **2015**, *4*, 245; e) K. Sumaru, T. Takagi, K. Morishita, T. Satoh, T. Kanamori, Soft matter 2018, 14, 5710; f) L. Li, J. M. Scheiger, P. A. Levkin, Adv. Mat. 2019, e1807333; g) A. M. Kloxin, A. M. Kasko, C. N. Salinas, K. S. Anseth, *Science* **2009**, *324*, 59.

[8] I. Tomatsu, K. Peng, A. Kros, *Adv. Drug Del. Rev.* **2011**, *63*, 1257.

[9] M. A. Azagarsamy, D. D. McKinnon, D. L. Alge, K. S. Anseth, *ACS Macro Lett.* **2014**, *3*, 515.

[10] B. D. Fairbanks, S. P. Singh, C. N. Bowman, K. S. Anseth, *Macromol.* **2011**, *44*, 2444.

[11] T. L. Rapp, C. B. Highley, B. C. Manor, J. A. Burdick, I. J. Dmochowski, *Chem. Eur. J.* **2018**, *24*, 2328.

[12] a) T. Çaykara, O. Güven, *Pol. Degrad. Stab.* **1999**, *65*, 225; b) H. Kaczmarek, A. Kamińska, A. van Herk, *Europ. Pol. J.* **2000**, *36*, 767; c) C. Wochnowski, M. A. Shams Eldin, S. Metev, *Pol. Degrad. Stab.* **2005**, *89*, 252.

[13] A. Torikai, M. Ohno, K. Fueki, *J. Appl. Polym. Sci.* **1990**, *41*, 1023.

[14] C. A. Bonino, J. E. Samorezov, O. Jeon, E. Alsberg, S. A. Khan, *Soft Matter* **2011**, *7*, 11510.

[15] a) A. Torikai, M. Ohno, K. Fueki, *J. Appl. Polym. Sci.* **1990**, *41*, 1023; b) T. Mitsuoka, A. Torikai, K. Fueki, *J. Appl. Polym. Sci.* **1993**, *47*, 1027.

[16] O. Chiantore, L. Trossarelli, M. Lazzari, *Polymer* **2000**, *41*, 1657.

[17] R. W. Johnstone, I. G. Foulds, M. Parameswaran, *J. Vac. Sci. Technol. B* **2008**, *26*, 682.

[18] R. Shanti, A. N. Hadi, Y. S. Salim, S. Y. Chee, S. Ramesh, K. Ramesh, *RSC Adv.* **2017**, *7*, 112.

[19] H. Kaczmarek, A. Kamińska, A. van Herk, *Europ. Pol. J.* **2000**, *36*, 767.

[20] N. Grassie, *P. Appl. Chem.* **1973**, *34*, 247.

[21] C. Wochnowski, M. A. Shams Eldin, S. Metev, *Pol. Degrad. Stab.* **2005**, *89*, 252.

[22] T. Çaykara, O. Güven, *Pol. Degrad. Stab.* **1999**, *65*, 225.

[23] a) C. R. Becer, S. Hahn, M. W. M. Fijten, H. M. L. Thijs, R. Hoogenboom, U. S. Schubert, *J. Polym. Sci. A Polym. Chem.* **2008**, *46*, 7138; b) P. J. Roth, F. D. Jochum, F. R. Forst, R. Zentel, P. Theato, *Macromol.* **2010**, *43*, 4638.

[24] Y. Du, E. Lo, S. Ali, A. Khademhosseini, *Proc. Natl. Acad. Sci. U.S.A* **2008**, *105*, 9522.

[25] G. C. Le Goff, R. L. Srinivas, W. A. Hill, P. S. Doyle, *Eur. Pol. J.* **2015**, *72*, 386.

[26] N. Doshi, A. S. Zahr, S. Bhaskar, J. Lahann, S. Mitragotri, *Proc. Natl. Acad. Sci. U.S.A* **2009**, *106*, 21495.

[27] M. Chen, L. Zhou, Y. Guan, Y. Zhang. *Angew. Chem. Int. Ed.* **2013,** *52*, 9961-9965.

[28] B. Xue, V. Kozlovskaya, E. Kharlampieva. *J. Mater. Chem. B* **2017,** *5*, 9-35.

[29] J. Thiele, Y. Ma, S. M. C. Bruekers, S. Ma, W. T. S. Huck. *Adv. Mater.* **2014,** *26*, 125-148.

[30] O. Guillame-Gentil, O. Semenov, A. S. Roca, T. Groth, R. Zahn, J. Vörös, M. Zenobi-Wong. *Adv. Mater.* **2010,** *22*, 5443-5462.

[31] H. Otsuka, Y. Nagasaki, K. Kataoka. *Adv. Drug Deliv. Rev.* **2012,** *64*, 246-255.

[32] D. Fayol, G. Frasca, C. Le Visage, F. Gazeau, N. Luciani, C. Wilhelm. *Adv. Mater.* **2013,** *25*, 2611-2616.

[33] T. Tronser, A. A. Popova, M. Jaggy, M. Bastmeyer, P. A. Levkin. *Adv. Healthc. Mater.* **2017,** *6*, 1700622-1700630.

ToC

Hydrogels are soft materials relevant for research and industry. Their surface- and microstructure are decisive properties for their respective application. Herein, a UV based method to structure hydrogels is introduced, which comprises experimental simplicity and versatile applicability by exploiting the inherent photodegradability of hydrophilic polymethacrylates. The biocompatibility of such microstructured hydrogels is shown for cell culture experiments.

Keyword hydrogels

Lei Li, Johannes M. Scheiger, Tina Tronser, Connor Long, Konstantin Demir, Christina L. Wilson, and Pavel A. Levkin*

Title Inherent Photodegradability of Polymethacrylate Hydrogels: Straightforward Access to Microstructures and Particles

ToC figure ((Please choose one size: 55 mm broad × 50 mm high))